A FLAT-PULSE ANALYTIC FRAMEWORK FOR MODELING INVERSE COMPTON SCATTERING AND PONDEROMOTIVE BROADENING *

E. Breen†[1], E. Rogers[1], G. Krafft[1,2], B. Terzić[1]
[1]Old Dominion University, Norfolk, USA
[2]Jefferson Lab, Newport News, USA

Abstract

We present a new general analytic formula for radiation spectra from inverse Compton scattering with a flat laser pulse at an arbitrary scattering angle. Using the analytic solution for a flat laser pulse, we build an approximation of a Gaussian pulse as a series of flat pulses with varying field strengths. From this description we obtain an expression for the phase modulation between successive flat pulses due to changing field strength, which produces ponderomotive broadening in the scattered spectra.

INTRODUCTION

Inverse Compton scattering (ICS) is a promising mechanism for generating compact, high-brightness x-ray and gamma-ray sources. In ICS, photons from a laser pulse collide with relativistic electrons and are upshifted in frequency through relativistic Doppler effects. Modern ICS systems operate in regimes where nonlinear interactions between the laser field and electron motion become significant, producing harmonic generation and ponderomotive broadening in the scattered spectrum.

Accurate modeling of these spectral effects generally requires detailed numerical calculations of the electron trajectory inside the laser field. While several numerical approaches exist, analytic or semi-analytic methods remain valuable because they provide physical insight into the scattering process and can substantially reduce computational cost.

In this work, we present a new analytic framework that approximates an arbitrary laser pulse envelope as a sequence of flat laser pulses. Exact solutions for radiation generated by flat pulses are then combined coherently with phase corrections between successive pulse segments. This approach reproduces nonlinear spectral broadening while preserving much of the simplicity of the analytic flat-pulse solution.

ANALYTIC SCATTERED SPECTRUM FOR A FLAT LASER PULSE

Calculating the scattered spectrum in inverse Compton scattering requires calculating the effective motion of the electron as it passes through the laser pulse. In the linear and nonlinear regimes, as well as both the Thomson and Compton regimes, this requires computing [1]

$$\begin{aligned} D_1(\omega') &= \frac{1}{\gamma(1-\beta\cdot\hat{k})}\int \tilde{A}(\xi')\, e^{i\Phi(\xi')}d\xi', \\ D_2(\omega') &= \frac{1}{\gamma^2(1-\beta\cdot\hat{k})^2}\int \frac{\tilde{A}^2(\xi')}{2} e^{i\Phi(\xi')}d\xi', \\ \Phi(\xi') &= \frac{\omega'}{c}\left(\begin{array}{c} \xi'\frac{(1-\beta\cdot\hat{k}')}{(1-\beta\cdot\hat{k})} - I_2\int_{-\infty}^{\xi'}\tilde{A}(\xi'')d\xi'' \\ +I_1\int_{-\infty}^{\xi'}\tilde{A}^2(\xi'')d\xi'' \end{array}\right), \end{aligned} \tag{1}$$

$$\begin{aligned} I_1 &= \frac{1-\hat{k}\cdot\hat{k}'}{2\gamma^2(1-\beta\cdot\hat{k})^2}, \\ I_2 &= \left(\frac{\beta\cdot\varepsilon}{(1-\beta\cdot\hat{k})}(1-\hat{k}\cdot\hat{k}') - \hat{k}'\cdot\varepsilon\right)\frac{1}{\gamma(1-\beta\cdot\hat{k})}, \end{aligned} \tag{2}$$

where β is the initial electron velocity vector divided by the speed of light, $\hat{k}$ and $\hat{k}'$ are the unit vector incident and scattered photon directions, ϵ is the polarization of the incident laser, and $\tilde{A}$ its normalized vector potential

$$\tilde{A}(\xi) = a(\xi)\cos\left(\frac{2\pi\xi}{\lambda}\right). \tag{3}$$

The spectrum is then computed from these expressions [2].

For a flat pulse laser envelope with strength a and with N full periods with wavelength λ, $\tilde{A}(\xi) = a[\Theta(\xi + N\lambda/2) - \Theta(\xi - N\lambda/2)]$, these integrals can be evaluated exactly in terms of Bessel functions, just as in case of undulators [3]

$$\begin{aligned} D_1(\omega') = &\frac{a e^{i\frac{\omega'}{c}\Phi_c}}{\gamma(1-\beta\cdot\hat{k})} \\ &\times\sum_{n=0}^{\infty}\frac{\sin((\frac{\omega'}{cQ(a)}-\frac{2\pi n}{\lambda})\frac{N\lambda}{2})}{\frac{\omega'}{cQ(\theta)}-\frac{2\pi n}{\lambda}}G_x^n(\omega'), \end{aligned} \tag{4}$$

$$\begin{aligned} D_2(\omega') = &\frac{a^2 e^{i\frac{\omega'}{c}\Phi_c}}{2\gamma^2(1-\beta\cdot\hat{k})^2} \\ &\times\sum_{n=-\infty}^{\infty}\frac{\sin((\frac{\omega'}{cQ(a)}-\frac{2\pi n}{\lambda})\frac{N\lambda}{2})}{\frac{\omega'}{cQ(\theta)}-\frac{2\pi n}{\lambda}}G_z^n(\omega'), \end{aligned} \tag{5}$$

where the phase term, Φ_c, is constant

$$\Phi_c = I_2\frac{a\lambda}{2\pi}\sin(\pi N) + I_1\left(\frac{a^2\lambda}{8\pi}\sin(2\pi N) + \frac{a^2}{4}N\lambda\right). \tag{6}$$

We define expressions for the Bessel function component

* Work supported by the NSF CAREER grant No. 1847771 and the NSF CSSI grant No. 2513760, and by Jefferson Science Associates, LLC under U.S. DOE Contract No. DE-AC05-06OR23177.
† ebree001@odu.edu

PREPRINT

$$G_x^n(\omega') = \sum_{j=-\infty}^{\infty} J_{\ell_x}\left(I_2\frac{a\lambda\omega'}{2\pi c}\right)\times\left[(-1)^{\frac{\ell_x+n-1}{2}}\left(J_{\frac{\ell_x+n-1}{2}}\left(I_1\frac{a^2\lambda\omega'}{8\pi c}\right)-J_{\frac{\ell_x+n+1}{2}}\left(I_1\frac{a^2\lambda\omega'}{8\pi c}\right)\right)\right.$$
$$\left.+\,J_{\frac{n-\ell_x-1}{2}}\left(I_1\frac{a^2\lambda\omega'}{8\pi c}\right)+J_{\frac{n-\ell_x+1}{2}}\left(I_1\frac{a^2\lambda\omega'}{8\pi c}\right)\right], \tag{7}$$

$$G_z^n(\omega') = \sum_j (-1)^{\frac{\ell_z+n-1}{2}} J_{\ell_z}\left(I_2\frac{a\lambda\omega'}{2\pi c}\right)\times\left[2J_{\frac{\ell_z+n}{2}}\left(I_1\frac{a^2\lambda\omega'}{8\pi c}\right)-J_{\frac{\ell_z+n-2}{2}}\left(I_1\frac{a^2\lambda\omega'}{8\pi c}\right)-J_{\frac{\ell_z+n+2}{2}}\left(I_1\frac{a^2\lambda\omega'}{8\pi c}\right)\right.$$
$$\left.+\,2J_{\frac{\ell_z-n}{2}}\left(I_1\frac{a^2\lambda\omega'}{8\pi c}\right)-J_{\frac{\ell_z-n-2}{2}}\left(I_1\frac{a^2\lambda\omega'}{8\pi c}\right)-J_{\frac{\ell_z-n+2}{2}}\left(I_1\frac{a^2\lambda\omega'}{8\pi c}\right)\right], \tag{8}$$

where, in order to preserve the appropriate parity relationships, we have defined $\ell_x = n-1+2j$ and $\ell_z = n+2j$, and finally

$$Q(a) = \frac{(1-\beta\cdot\hat{k}')}{(1-\beta\cdot\hat{k})} + \frac{a^2}{2}I_1. \tag{9}$$

The spectrum is a series of harmonics with peaks located at frequencies

$$\omega_n' = n\frac{2\pi c}{\lambda Q(a)}, \tag{10}$$

where n is the harmonic number.

SCATTERED SPECTRUM OF A SERIES OF FLAT PULSES

Let $\tilde{A}(\xi)$ be a series of $\mathcal{N}$ flat laser pulses of equal wavelengths and periods with varying field strengths with endpoints ξ_i

$$\tilde{A}(\xi) = \sum_i^{\mathcal{N}} a_i \cos\left(\frac{2\pi\xi}{\lambda}\right)[\Theta(\xi_{i-1}+N\lambda/2)-\Theta(\xi_i-N\lambda/2)]. \tag{11}$$

An incident laser pulse envelope can then be approximated using a series of flat pulses as shown in Fig. 1. It follows that for any number of flat pulses with normalized vector potentials $\tilde{A}_i$

$$D_1(\omega') = \sum_i^{\mathcal{N}} D_{1,i}(\omega')\, e^{i\Phi_{p,i}}, \tag{12}$$

$$D_2(\omega') = \sum_i^{\mathcal{N}} D_{2,i}(\omega')\, e^{i\Phi_{p,i}}, \tag{13}$$

where $D_{1,i}$ and $D_{2,i}$ are the solutions for a single flat pulse with normalized amplitude a_i, and $\Phi_{p,i}$ is defined momentarily. The phase for the i-th pulse obtained from Eq. (1) is

$$\Phi_i(\xi') = \frac{\omega'}{c}\begin{pmatrix} \xi'\frac{(1-\beta\cdot\hat{k}')}{(1-\beta\cdot\hat{k})} \\ -I_2\sum_{j=0-\infty}^{i}\int^{\xi'}\tilde{A}_j(\xi''))\,d\xi'' \\ +I_1\sum_{j=0-\infty}^{i}\int^{\xi'}\tilde{A}_{j^2}(\xi'')\,d\xi'' \end{pmatrix}. \tag{14}$$

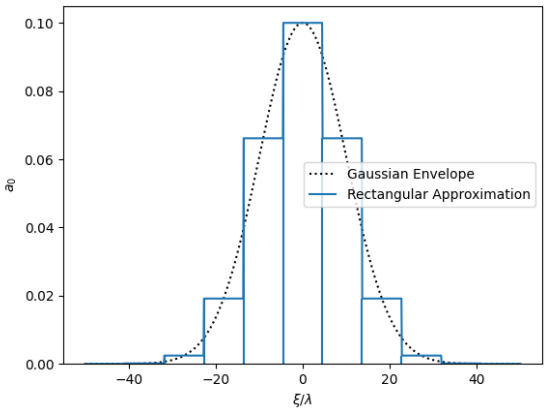

Figure 1: A Gaussian laser pulse approximated by $\mathcal{N} = 11$ flat pulses with equal temporal width. Increasing the number of divisions, $\mathcal{N}$, improves reconstruction of the original envelope and corresponding radiation spectrum.

Thus the solution for a series of flat pulses is the sum of the solutions for a single flat pulse with an additional phase term which modulates the result based on the changing values a_i,

$$\Phi_i(\xi') = \Phi_{R,i}(\xi') + \Phi_{p,i}, \tag{15}$$

where

$$\Phi_{R,i}(\xi') = \frac{\omega'}{c}\begin{pmatrix} \xi' Q(a_i) - I_2\frac{a_i\lambda}{2\pi}\sin\left(\frac{2\pi\xi}{\lambda}\right) \\ +I_1\frac{a_i^2\lambda}{8\pi}\sin\left(\frac{4\pi\xi}{\lambda}\right)+I_2\frac{a_i\lambda}{2\pi}\sin\left(\frac{2\pi\xi_{i-1}}{\lambda}\right) \\ -I_1\frac{a_i^2\lambda}{8\pi}\sin\left(\frac{4\pi\xi_{i-1}}{\lambda}\right)-I_1\frac{a^2}{2}\xi_{i-1} \end{pmatrix}, \tag{16}$$

$$\Phi_{p,i} = \frac{\omega'}{c}\sum_{j=0}^{i-1}\begin{pmatrix} I_1\frac{a_j^2}{2}(\xi_j-\xi_{j-1}) \\ -I_2\frac{a_j\lambda}{2\pi}\left(\sin\left(\frac{2\pi\xi_j}{\lambda}\right)-\sin\left(\frac{2\pi\xi_{j-1}}{\lambda}\right)\right) \\ +I_1\frac{a_j^2\lambda}{8\pi}\left(\sin\left(\frac{4\pi\xi_j}{\lambda}\right)-\sin\left(\frac{4\pi\xi_{j-1}}{\lambda}\right)\right) \end{pmatrix}. \tag{17}$$

This phase term $\Phi_{p,i}$ introduces a relative phase shift between contributions from each pulse segment. This effect, combined with the shift in the harmonic location with a_i in Eq. (10), creates ponderomotive broadening in the spectrum. For any particular harmonic n, each $D_{1,i}$ and $D_{2,i}$

PREPRINT

contributes a peak. The larger the difference in a_i values, the further apart these harmonics of the same number become, broadening the spectrum.

The flat-pulse approximation was compared against spectra generated using the SENSE [1] simulation framework as shown in Fig. 2. In the linear scattering regime (illustrated here with the $a_0 = 0.1$ case), the approximation converges rapidly as the number of flat pulses is increased. Even a modest number of pulse segments reproduces the spectral shape and harmonic structure obtained numerically. In the

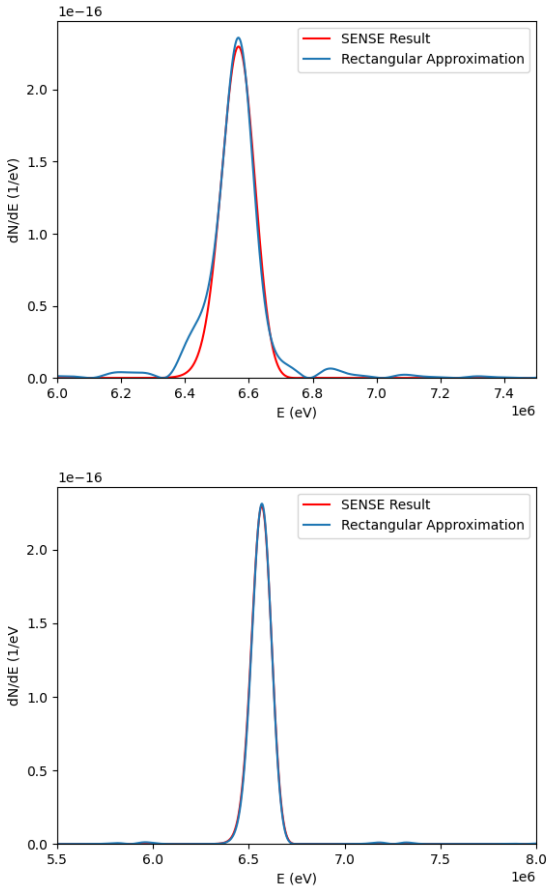

Figure 2: Spectra calculated with the flat pulse approximation method in the linear scattering regime quickly converge to the result produced by SENSE with increased rectangular divisions. In these figures $a = 0.1$, and the spectrum is approximated with (left) $\mathcal{N} = 5$ flat pulses and (right) $\mathcal{N} = 15$ flat pulses.

nonlinear regime (illustrated here with the $a_0 = 1$ case), additional pulse divisions are required because the pulse envelope is more sharply peaked and the harmonic frequencies vary more significantly across it, as shown in Fig. 3. Nevertheless, the flat-pulse model accurately reproduces the broadened fundamental harmonic associated with ponderomotive effects. The results demonstrate that the method captures the essential physics of nonlinear ICS spectra while remaining computationally efficient. Because the model is based on analytic flat-pulse solutions, it also provides direct

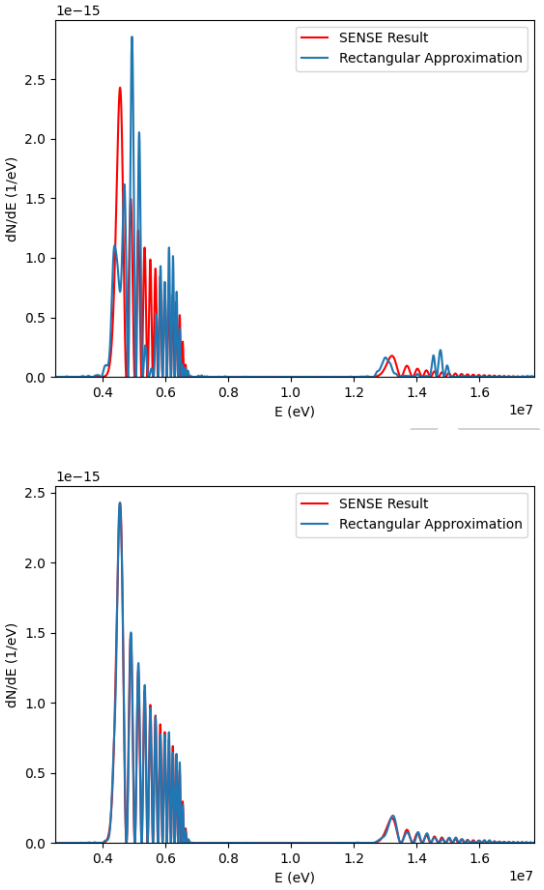

Figure 3: Spectra in the nonlinear scattering regime require a larger number of rectangular divisions in the flat pulse approximation, as the laser pulse is more sharply peaked. Here $a = 1$, and the spectrum is approximated with (left) $\mathcal{N} = 15$ pulses and (right) $\mathcal{N} = 45$ pulses. The nonlinear spectrum shows ponderomotive broadening in the fundamental harmonic, which is accurately replicated by the flat pulse approximation.

physical interpretation of how pulse shape and field strength influence spectral broadening.

CONCLUSION

We have developed a new analytic framework for modeling inverse Compton scattering using a sequence of flat laser pulses to approximate an arbitrary laser envelope. By coherently combining exact flat-pulse solutions with phase modulation terms between adjacent pulse segments, the model reproduces nonlinear spectral broadening and ponderomotive effects observed in ICS spectra. The approach provides a flexible and computationally efficient alternative to fully numerical calculations and may be extended to more general scattering geometries and laser pulse profiles. Future work will investigate applications to strongly nonlinear scattering regimes and radiation reaction effects.

PREPRINT

REFERENCES

[1] G. A. Krafft, B. Terzić, E. Johnson, and G. Wilson, "Scattered spectra from inverse compton sources operating at high laser fields and high electron energies", *Phys. Rev. Accel. Beams*, vol. 26, p. 034401, Mar. 2023. doi:10.1103/PhysRevAccelBeams.26.034401

[2] B. Terzić, J. McKaig, E. Johnson, T. Dharanikota, and G. A. Krafft, "Laser chirping in inverse compton sources at high electron beam energies and high laser intensities", *Phys. Rev. Accel. Beams*, vol. 24, p. 094401, Sep. 2021. doi:10.1103/PhysRevAccelBeams.24.094401

[3] E. Esarey, S. K. Ride, and P. Sprangle, "Nonlinear Thomson scattering of intense laser pulses from beams and plasmas", *Phys. Rev. E*, vol. 48, pp. 3003–3021, Oct. 1993. doi:10.1103/PhysRevE.48.3003

PREPRINT